

***p*-doped single-quantum-well infrared photodetector**

K. M. S. V. Bandara, B. F. Levine, and J. M. Kuo
 AT&T Bell Laboratories, Murray Hill, New Jersey 07974
 (Received 20 April 1993)

We report detailed optical, electrical, and transport measurements on *p*-doped single-quantum-well infrared photodetectors. We find that the properties of these single *p*-type structures are substantially different from those of *n*-type single-well detectors.

Although there have been extensive studies¹⁻⁸ of multiple-quantum-well infrared photodetectors (QWIP's), relatively little research has been performed on detectors consisting of only a single quantum well.⁹⁻¹¹ One of these studies¹¹ found strikingly different behavior between multiple-well and single-well photodetectors in *n*-type material. In this investigation we report optical, electrical, and transport measurements of *p*-doped¹² single QWIP's.

The structure, schematically shown in Fig. 1(a), was grown on a semi-insulating GaAs substrate via gas source molecular-beam epitaxy, and consisted of a single *p*-doped ($p = 2 \times 10^{18} \text{ cm}^{-3}$ with Be) $L_w = 40 \text{ \AA}$ quantum well surrounded by two $L_b = 300 \text{ \AA}$ undoped $\text{Al}_{0.3}\text{Ga}_{0.7}\text{As}$ barriers. The GaAs contact layers (top $\frac{1}{2} \mu\text{m}$ and bottom $1 \mu\text{m}$) were also *p* doped to the same carrier density. The dark current I_d (measured at $T = 77 \text{ K}$) and the photocurrent (measured at $T = 10 \text{ K}$) produced by $T = 300 \text{ K}$ background illumination through the Dewar window are shown in Fig. 2. Note that the curves are quite symmetrical with bias voltage, indicating that the Be dopant did not significantly diffuse out of the

quantum well.

The responsivity was measured at *normal incidence*¹² since the strong mixing between the light and heavy holes at $k \neq 0$ allows this advantageous geometry. The resulting spectrum is shown in Fig. 3 for a bias of $V_b = -0.4 \text{ V}$ (i.e., mesa top negative), and was found to be independent of temperature from $T = 10$ to 80 K to within experimental error ($< 10\%$). The peak position $\lambda_p = 7.2 \mu\text{m}$ as well as the absolute magnitude of the responsivity are, as expected, quite similar to those of a previously discussed¹² 50-period *p*-QWIP having the same values of $L_w = 40 \text{ \AA}$, $L_b = 300 \text{ \AA}$, and $\text{Al}_{0.3}\text{Ga}_{0.7}\text{As}$ barrier composition. The bias dependence of the responsivity is shown in Fig. 4 as the solid curve together with that of the previously measured¹¹ single *n*-QWIP (shown as the dashed curve) for comparison. Note that the *p*-QWIP responsivity increases approximately linearly with bias at low voltage demonstrating the *bound-to-continuum*⁸ nature of the intersubband transition, whereas the *n*-QWIP requires a large bias offset (i.e., the responsivity is essentially zero for $V_b < 0.1 \text{ V}$). In addition, for the *p*-QWIP there is no saturation of the responsivity with increasing bias even for very large voltages of $V_b = -0.5 \text{ V}$ (i.e., a voltage drop per barrier of -0.25 V corresponding to 12.5 V for a 50-period QWIP). This is also strikingly different from

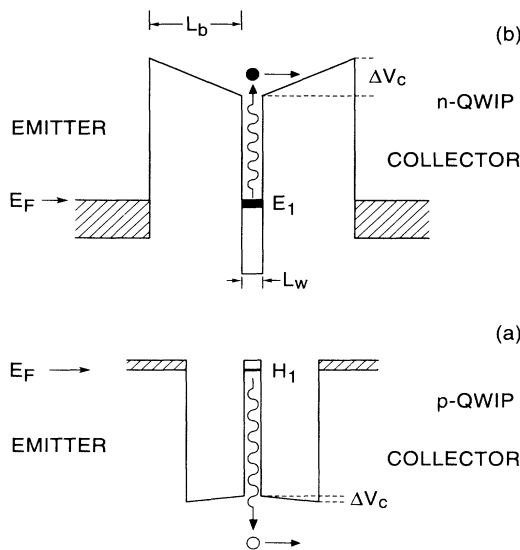


FIG. 1. (a) Schematic valence-band diagram of a single *p*-doped QWIP. The ground-state heavy-hole energy level is indicated as H_1 . (b) Conduction-band diagram of a single *n*-type QWIP. The ground-state electron level is indicated as E_1 . The Fermi levels are E_F , and the barrier band bending is ΔV_c .

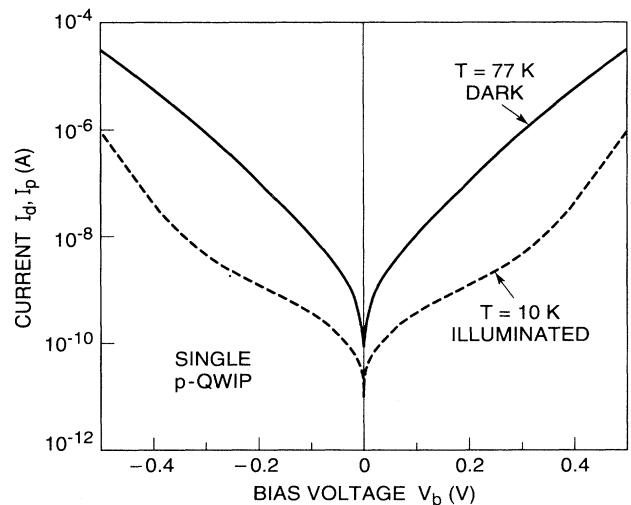


FIG. 2. Dark current I_d (at $T = 77 \text{ K}$), and photocurrent I_p (at $T = 10 \text{ K}$) as a function of bias voltage for a $200\text{-}\mu\text{m}$ -diam QWIP. (Positive bias means mesa top positive.)

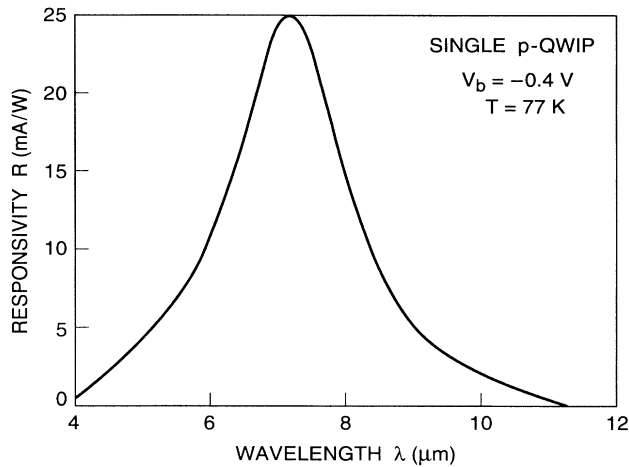


FIG. 3. Responsivity spectrum measured at $V_b = -0.4$ V and $T = 77$ K.

that of the n -QWIP. These significant differences will be discussed after presenting the p -QWIP experimental data.

In order to better understand this single p -QWIP responsivity behavior, we measured the current noise at $T = 77$ K and obtained the gain shown in Fig. 5 using $i_n = \sqrt{4eI_d g \Delta f}$. Note that the gain increases monotonically with increasing bias, thereby explaining the similar increase of the responsivity with bias in Fig. 4. That is, the responsivity and gain of this single-well p -QWIP both behave as the 50-period p -QWIP (Ref. 12) [i.e., not as the single-well n -QWIP (Ref. 11)]. The gain can be analyzed further in terms of the quantum-well capture probability p_c , which is related to the optical gain g by $g = (1 - p_c) / N p_c$, where N is the number of quantum wells. Thus, for a single-well $N = 1$ and $p_c = (1 + g)^{-1}$ which has been plotted (as the solid curve) in Fig. 6 using the gain from Fig. 5. At zero bias the capture probability

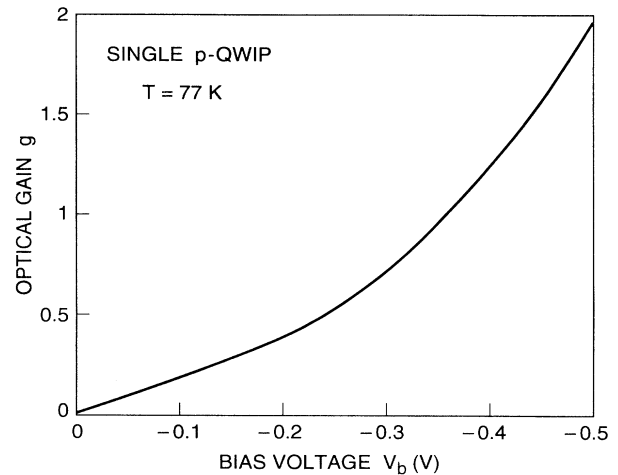


FIG. 5. Optical gain vs bias voltage measured at $T = 77$ K.

is $p_c = 100\%$ and decreases monotonically with increasing bias reaching $p_c = 34\%$ at $V_b = -0.5$ V. (Also shown in the same figure for comparison we have included the previously measured¹¹ single-well n -doped QWIP to be discussed later.) The reason for this decrease in p_c for the p -QWIP is that as the electric field increases the carrier velocity increases and thus the transit time across the well decreases.

In addition to the capture probability p_c , we can now also determine the quantum-well escape probability⁸ p_e . The peak responsivity R_p can be expressed in terms of p_e as

$$R_p = (e/h\nu)\eta_a p_e g, \quad (1)$$

where $\eta_a = (1 - e^{-2al})$ is the two-pass unpolarized

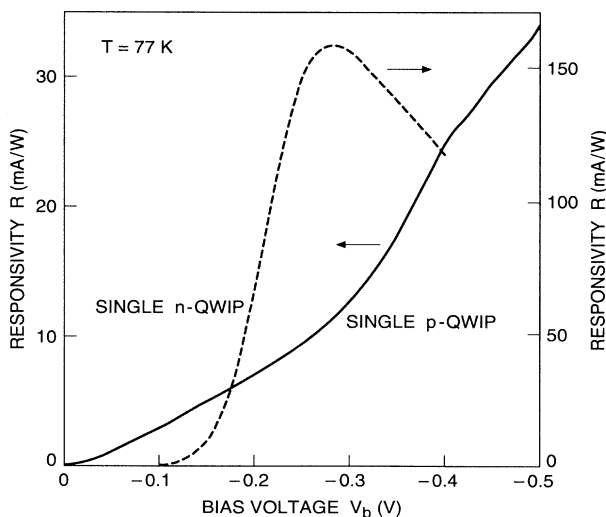


FIG. 4. Responsivity vs bias voltage measured at $\lambda_p = 7.2$ μm and $T = 77$ K. The solid curve is for the p -QWIP (left-hand scale) while the dashed curve is for a previously measured ($T = 12$ K) n -QWIP (right-hand scale).

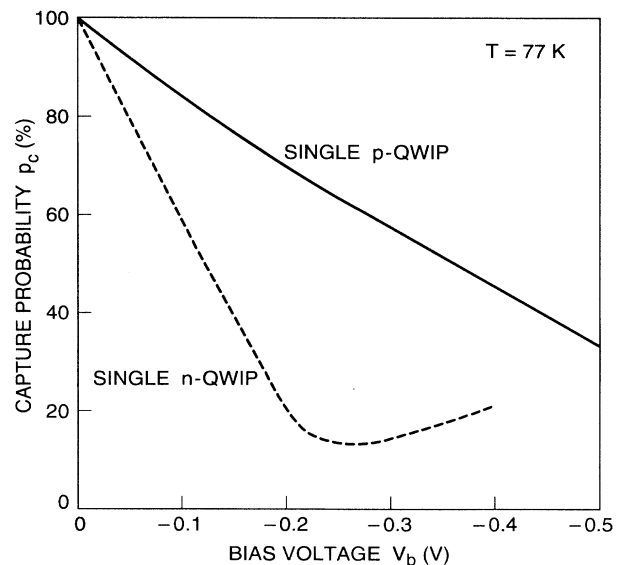


FIG. 6. Capture probability p_c as a function of bias voltage measured at $T = 77$ K. The solid curve is for the single p -QWIP. The dashed line is for a previously measured single n -QWIP.

normal-incidence absorption quantum efficiency. Thus, using the bias dependences of the responsivity $R_p(V_b)$ from Fig. 4 and the optical gain $g(V_b)$ from Fig. 5 we can experimentally determine $p_e(V_b)$. For this purpose we use $\eta_a = 0.4\%$. This was obtained by scaling the 50-period p -QWIP value¹² of η_a (50 QW's) $\sim 20\%$ by the number of wells and also by the doping density which was $N_D = 4 \times 10^{18} \text{ cm}^{-3}$ for the 50 quantum-well sample and only $2 \times 10^{18} \text{ cm}^{-3}$ for the single-well p -QWIP. We have also corrected for the factor of 2 enhancement¹³ of the optical intensity (and, hence, absorption) due to the single quantum well being at the position of maximum optical field (i.e., at $\lambda'/4$ where λ' is the wavelength in the semiconductor). Substituting this value for η_a in Eq. (1) we obtain $p_e \approx 75\%$ for all biases and thus the photoexcited hole can readily escape from the quantum well.

We have now determined the important optical, electrical, and transport parameters for the single-well p -QWIP (i.e., the responsivity spectrum and bias dependence, the current-voltage curves, the optical gain, as well as the quantum-well capture and escape probabilities), and are thus now in a position to discuss the significant differences with single n -QWIP's. We first explain the lack of a responsivity bias offset for p -QWIP's (shown in Fig. 4). As indicated in Fig. 1, the n -QWIP ($L_w = 40 \text{ \AA}$, $L_b = 500 \text{ \AA}$ of $\text{Al}_{0.3}\text{Ga}_{0.7}\text{As}$ and $N_D = 1 \times 10^{18} \text{ cm}^{-3}$) has a much stronger band bending of the barriers than the p -QWIP. This is a result of the larger hole effective-mass m_h^* relative to the electron mass m_e^* and the consequent small ground-state hole energy $H_1 = 25 \text{ meV}$ [in Fig. 1(a)] with respect to the ground-state electron energy $E_1 = 88 \text{ meV}$ [in Fig. 1(b)]. That is, the alignment of the Fermi level in the doped quantum well with the Fermi levels in the emitter and collector contact layers requires a large drop in the E_1 electron level (and thus a substantial barrier band bending) whereas for H_1 this adjustment is much less. Using a self-consistent theory, we have calculated¹¹ that the barrier band bending for the simple n -QWIP is $\Delta V_c = 50 \text{ meV}$ whereas it is only $\Delta V_c = 15 \text{ meV}$ for the p -QWIP discussed above. Furthermore (due to the $k \neq 0$ valence-band hole intersubband selection rules), the responsivity peak at $\lambda_p = 7.2 \mu\text{m} =$

172 meV is sufficiently high in the *continuum* ($\Delta E = 22 \text{ meV}$) above the $V_b = 150 \text{ meV}$ barrier height that $\Delta E > \Delta V_c$. In strong contrast, the n -QWIP band bending of $\Delta V_c = 50 \text{ meV}$ is so large that the photoexcited electron ($\Delta E = 13 \text{ meV}$) remains *bound* (i.e., $\Delta E < \Delta V_c$) and thus cannot escape without a large applied bias voltage to eliminate ΔV_c . That is, for the p -QWIP, p_e is large even at low bias and thus remains essentially constant as the bias is increased, where for the n -QWIP p_e is very small at low V_b and thus requires a substantial bias to overcome the band bending ΔV_c and allow the photoexcited electrons to escape.

The other important difference shown in Fig. 4 is the continuing increase of the p -QWIP responsivity with bias, while the n -QWIP reaches a maximum after which it strongly decreases with increasing bias. This n -QWIP maximum was found¹¹ to be due to a maximum in the gain, i.e., a minimum in the well capture probability p_c versus bias voltage as shown by the dotted curve in Fig. 6. In contrast, the p -QWIP capture probability continues to decrease monotonically with bias. This difference is again a result of the large hole effective mass m_h^* . For both n - and p -QWIP's the initial decrease in p_c is due to the decrease in the photoexcited carrier transit time across the quantum well. However, at high bias the n -QWIP capture probability increases due to direct tunneling¹⁴ of the low m_e^* electrons from the emitter contact which effectively "short circuits" the hot carrier transport process. For high-mass holes this direct tunneling process is inhibited and thus the capture probability continues to decrease as shown in Fig. 6 (i.e., the gain continues to increase in Fig. 5).

In summary, we have presented optical, electrical, and transport measurements of single-quantum-well p -QWIP's. The bias behavior of the responsivity, optical gain, quantum-well escape probability, and quantum-well capture probability were found to be strikingly different from that of single-well n -QWIP's, as a result of the large hole effective-mass m_h^* relative to the electron mass m_e^* .

We would like to acknowledge J. de Jong for help with the metallization process.

¹B. F. Levine, C. G. Bethea, G. Hasnain, V. O. Shen, E. Pelve, R. R. Abbott, and S. J. Hsieh, *Appl. Phys. Lett.* **56**, 851 (1990).

²B. F. Levine, in *Advanced Research Workshop on Intersubband Transitions in Quantum Wells*, Vol. 288 of *NATO Advanced Study Institute, Series B: Physics*, edited by E. Rosencher, B. Vinter, and B. F. Levine (Plenum, New York, 1992), p. 43.

³J. Y. Andersson and L. Lundqvist, *Appl. Phys. Lett.* **59**, 857 (1991).

⁴B. K. Janousek, M. J. Daugherty, W. L. Bloss, M. L. Rosenbluth, M. J. O'Loughlin, H. Kanter, F. J. De Luccia, and L. E. Perry, *J. Appl. Phys.* **67**, 7608 (1990).

⁵S. R. Andrews and B. A. Miller, *J. Appl. Phys.* **70**, 993 (1991).

⁶B. F. Levine, C. G. Bethea, K. G. Glogovsky, J. W. Stayt, and R. E. Leibenguth, *Semicond. Sci. Technol.* **6**, C114 (1991).

⁷L. J. Kozlowski, G. M. Williams, G. J. Sullivan, C. W. Farley, R. J. Anderson, J. K. Chen, D. T. Cheung, W. E. Tennant,

and R. E. DeWames, *IEEE Trans. Electron. Devices* **38**, 1124 (1991).

⁸B. F. Levine, A. Zussman, S. D. Gunapala, M. T. Asom, J. M. Kuo, and W. S. Hobson, *J. Appl. Phys.* **72**, 4429 (1992).

⁹H. C. Liu, G. C. Aers, M. Buchanan, Z. R. Wasilewski, and D. Landheer, *J. Appl. Phys.* **70**, 935 (1991).

¹⁰E. Rosencher, F. Luc, Ph Bois, and S. Delaitre, *Appl. Phys. Lett.* **61**, 468 (1992).

¹¹K. M. S. V. Bandara, B. F. Levine, R. E. Leibenguth, and M. T. Asom, *J. Appl. Phys.* **74**, 1826 (1993).

¹²B. F. Levine, S. D. Gunapala, J. M. Kuo, S. S. Pei, and S. Hui, *Appl. Phys. Lett.* **59**, 1864 (1991).

¹³J. Y. Andersson and G. Landgren, *J. Appl. Phys.* **64**, 4123 (1988).

¹⁴K. M. S. V. Bandara, B. F. Levine, and M. T. Asom, *J. Appl. Phys.* **74**, 346 (1993).